数理解析研究所講究録
第677巻 1989年 220-244

Numerical Simulation of Collision of Liquid Droplets

東大・工 高橋 大輔 (Daisuke Takahashi)
東大・工 高見 穎郎 (Hideo Takami)

ABSTRACT

A new finite-difference method to compute the motion of fluid with free surfaces is propsed. This method is an improvement on the marker and cell method and by applying this one can recognize the configuration of fluid region including free surfaces with fewer memories by the rearrangement of markers. For three-dimensional calculation of the effect of surface tension, a statistical method is introduced; it can save the computational time much without loss of accuracy.

The computatinal results are shown for the case of splashing of a droplet, of collision of a droplet with a rigid wall and of collision of two droplets in axisymmetric, two-dimensional and three-dimensional situations.

I. INTRODUCTION

In recent years, there has been increasing interest in the analysis of the motion of the fluid with free surfaces. In particular, there are many interesting phenomena as for the action of small drops such as an ink jet or a milk crown.

The MAC (marker and cell) method[1] and the time-dependent grid generation method[2] are known as numerical methods simulating the fluid motion with free surfaces. The latter has an advantage that it is easy to determine the configuration of the free surface with high accuracy. However, it is difficult to apply this method in order to calculate great deformation, merging or splitting of the fluid because it is necessary to reform a grid system.

In general, the MAC method has a defect that it spends a lot of memories and much computational time to treat the free surface. Moreover, in a small scale motion, the surface tension plays an important role in a surface deformation. Therefore, few calculations were performed in the case of the large deformation or in a three-dimensional case.

We calculate the pressure at the surface by the curvature determined by the array of markers which approximate the configuration of the free surface and use fewer markers in the surface cell and rearrange them at each time step.

We can save memories and computational time with the above-mentioned tratement of the surface. Consequently, we can perform three-dimensional calculations more easily. In this paper, several motions of droplets are calculated in two-dimensional, axisymmetrical and three-dimensional cases by using the MAC method improved by us.

II. BASIC EQUATIONS AND NUMERICAL SCHEME OF SOLUTION

The governing equations which describe the motion of the fluid are the equation of continuity and the Navier-Stokes

equation. In the Cartesian coordinates, they are written as follows:

$$\nabla \cdot \mathbf{u} = 0, \tag{1}$$

$$\frac{\partial \mathbf{u}}{\partial t} + (\mathbf{u}\cdot\nabla)\mathbf{u} = -\nabla p + \nu\Delta\mathbf{u}, \tag{2}$$

where $\mathbf{u}$ is the velocity vector, p is the pressure and ν is the kinematic viscosity. By taking the divergence of the Navier-Stokes equation, we get the Poisson equation for the pressure:

$$\Delta p = -\frac{\partial D}{\partial t} - \nabla\cdot((\mathbf{u}\cdot\nabla)\mathbf{u}), \tag{3}$$

$$D = \nabla\cdot\mathbf{u}. \tag{4}$$

These equations are applied only in the fluid region.

In the finite-difference calculation, basic equations are approximated as follows:

$$\Delta p^n = \frac{D^n}{\Delta t} - \nabla\cdot((\mathbf{u}^n\cdot\nabla)\mathbf{u}^n), \tag{5}$$

$$\mathbf{u}^{n+1} = \mathbf{u}^n + \Delta t(-(\mathbf{u}^n\cdot\nabla)\mathbf{u}^n - \nabla p^n + \nu\Delta\mathbf{u}^{n+1}), \tag{6}$$

where Δt is the interval of time differencing and the index n denotes the number of the time step. The first term of the right hand side of eq.(5) is put in order to set $D^{n+1} = 0$.

For space differencing, all derivatives are approximated in the form of the central differencing.

On the free surface, there are surface boundary conditions and they are as follows:

$$\sigma_{ij} n_j = 0, \tag{7}$$

$$\sigma_{ij} = -p'\delta_{ij} + \nu\left(\frac{\partial u_j}{\partial x_i} + \frac{\partial u_i}{\partial x_j}\right), \tag{8}$$

$$p' = p + \gamma\left(\frac{1}{R_1} + \frac{1}{R_2}\right), \tag{9}$$

where γ is surface tension and R_1 and R_2 are the principal radii of curvature of the free surface which are positive when the center of curvature exists inside the fluid region and negative when it is outside the fluid region. As it is difficult to apply all conditions above in the finite-difference calculation, we only take account of a surface tension effect, the second term of the righthand side of eq.(9). The surface pressure is equal to $\gamma(1/R_1+1/R_2)$ and the velocity is extrapolated from the velocity inside the fluid region.

III. ALGORITHM OF CALCULATION

Using the basic equations, we simulate the fluid motion with the following algorithm (for simplicity, the situation is assumed to be two-dimensional). For example, the fluid region, the vacuum region and the wall are arranged as in Fig.1.a. The circular fluid region has the downward velocity by the gravity effect. We first make the regular mesh to the whole region (Fig.1.b). A unit of mesh is called "cell". The physical quantity of each cell is represented in its center. To approximate the fluid region, markers are placed as in Fig.1.c and they are assumed to move with the velocity of the fluid. It is important to place markers finely enough on the surface because the configuration of the surface is essential to determine the motion of the fluid. Then each cell is classified into empty(E), full(F), surface(S) and wall(W) cell. The rule of classification is as follows:

1) a cell in the wall region is W-cell.
2) a cell in which no marker exists is E-cell.
3) a cell in which some markers exist and which is adjacent to E-cell is S-cell.
4) the rest cell is F-cell.
5) Some of S-cells not adjacent to F-cell are renamed as E-cell.

The example of classification is shown in Fig.1.d. This classification roughly shows the configuration of the fluid region and each kind of cells are treated differently in the computation. The basic equations (5) and (6) are applied to F-cells and the boundary conditions are to S-cells. The slip conditions of walls are applied to W-cells adjacent to F-cells. No equations and no conditions are applied to E-cell because no fluid exists in it.

Finally, the procedure of computation is as follows:

0) At nth time step, markers are placed as they approximate

the configuration of the fluid region and the values of velocity are given to F-cells.

1) The principal radii of curvature are calculated from the positions of markers belonging to S-cells and the value of pressure of S-cells is calculated. The values of velocity are extrapolated from those of near-by F-cells.
2) Using eq.(5), the values of pressure of F-cells at nth time step are calculated by an iterative method.
3) Using eq.(6), the values of velocity of F-cells at (n+1)st time step are calculated by an iterative method.
4) Markers are moved with these velocity by a time interval Δt.
5) The configuration of the fluid region at (n+1)st time step is determined by the positions of markers and every cell is classified newly.
6) Return to the step 1).

After the calculation of large time steps using above procedure repeatedly, large deformation, merging or splitting of the fluid region may occur and the distribution of markers may become unbalanced. Then the configuration of fluid region can not be recognized exactly. It is necessary to rearrange markers on the basis of the positions of markers at the previous time step. As for S-cells, the markers are rearranged at every time step and the number of markers in each S-cell is always controlled. As for F-cells, the markers are necessary only when the configuration of the fluid region at the next time step is calculated and markers at the previous time step in F-cells need not be memorized.

The way of calculation of curvature from the positions of markers in S-cells is as follows. In two-dimensional or axisymmetrical cases, the curvature is easily calculated with the positions of three markers; one marker is selected from the S-cell in question and two markers are selected from adjacent S-cells. In three-dimensional case, the recognition of the curved free surface is very difficult and large amount of computation may be necessary. We avoid this problem by use of a

statistical method; four markers in the S-cell in question and adjacent S-cells determine a sphere uniquely which have those markers on its surface. The average of a reciprocal of the radius of spheres determined from all combinations of four markers is taken as an approximate value of the curvature. Such treatment leads to saving of the computational time.

IV. EXAMPLES OF CALCULATIONS

1. Splashing of a droplet

This example shows an axisymmetrical splashing of a droplet running into a pool of the same kind of fluid and a comparison with the experimental results of Macklin and Hobbs[3].

A droplet with 2.3mm diameter impacts a pool of 4mm depth at a velocity of 320cm/s. When a droplet strikes at the liquid surface of the pool, the surface caves in by the impact. Successively, the fluid near the cave concentrates and a liquid projection springs up consequently.

This calculation was already performed by Amsden and Harlow[4] but their calculation did not take account of the surface tension effect.

Numerical results are shown in Fig.2. In this figure, velocity vectors and pressure contours are plotted on respectively the left and right hand side of the symmetry axis. Also Fig.3 shows the dependence of the maximum height of the liquid region on the symmetry axis on time. The maximum projection height of experiment is about 10mm and calculational result is higher than experimental one. It is suspected that this difference is caused by the difference of the boundary condition of the pool.

Conditions used in this calculation are shown in Table 1.

2. Axisymmetrical collision of two droplets

In this example, a collision of two droplets is examined by changing the diameters and velocities of droplets.

Two droplets moving with the same speed in opposite directions collide coaxially. The calculations are performed by using cylindrical coordinates and the gravity effect is neglected.

Fig.4, Fig.5 and Fig.6 show the numerical results: surface configuration, velocity vector and pressure contours. In Fig.4, diameters of the two droplets are both 2.0mm and initial velocities in z-direction are $\pm$50cm/s respectively. In Fig.5, diameters of the droplets are 3.0mm and 1.5mm and initial velocities are $\pm$50cm/s. In Fig.6, diameters are 3.0mm and 1.5mm and initial velocities are $\pm$100cm/s.

In the case of Fig.4, two droplets merge into one body and expand in r-direction after the collision. Then velocity component in z-direction increases by the effect of surface tension. So the configuration of merged droplets which expanded restores.

Fig.5 shows that merged droplets first expand and then contract as in the former case. In the case of higher velocities (Fig.6), deformation in r-direction is greater than Fig.5, but the configuration is restored as above.

Conditions used in these calculations are shown in Table 2.

3. Collision of a droplet with a rigid wall

This example shows a collision of a droplet with a rigid wall. Calculations were performed for an axisymmetrical case and a two-dimensional case.

(1) axisymmetrical case

Calculations are performed for two values of surface tension, 75dyn/cm and 15dyn/cm, in the cylindrical coordinates and the numerical results are shown in Fig.7 and Fig.8 respectively. Gravity is neglected, diameter of the droplet is 2.2mm and initial velocity is 50cm/s in both figures. In the

case of Fig.7, the colliding droplet expands in r-direction. Then the droplet forms in a ring shape with a hole at the center by the effect of surface tension.

On the other hand, in the case of lower surface tension (Fig.8), the colliding droplet expands only so that the ring formation does not occur.

Conditions used in these calculations are shown in Table 3.

(2) two-dimensional case

These calculations are two-dimensional analyses of collisions with various collision angles.

Fig.9 and Fig.10 show the computatinal results with collision angle of 90^{o} and 45^{o}. Conditions in these calculations are shown in Table 4.

4. Three-dimensional collision of droplets

Fig.11 and Fig.12 show how two identical fluid spheres collide and merge with each other. All figures are drawn as a wire frame by removing hidden surfaces.

Fig.11 shows a head-on collision. After the collision, an asymmetrical frill appears and expands. It is suspected that this expansion is unstable and numerical error causes this instability. In the case of Fig.12, the direction of velocity vector is not parallel to the line which passes through centers of the spheres and merged spheres rotate around each other after collision. The effect of surface tension round off the projecting parts of the fluid occurred after the collision.

Conditions used in this calculation are shown in Table 5.

V. CONCLUSION

The improvement and the extension of MAC method was tried and axisymmetrical, two-dimensional and three-dimensional cases of fluid motions with free surfaces were calculated numerically. For this type of calculation, saving memories and computational time is an important problem. This problem is solved by putting markers only in surface cells sparsely and rearranging them at

each time step. In addition, a statistical method is used in order to calculate the effect of surface tension in the three-dimensional case. It saves computational time much and even the three-dimensional calculation becomes easier. Numerical results proposed in this paper are reasonable and they accord with actual observations well.

REFERENCE

1) Harlow, F. H. and Welch, J.E., Numerical calculation of time-dependent viscous incompressible flow of fluid with free surface. Phys. Fluids., 8(1965),pp.2182-2189.
2) Katano, Y., Kawamura, T. and Takami, H., Numerical study of drop formation from a capillary jet using a general coordinate system. Theoretical and Applied Mechanics, Vol.34(Univ. Tokyo Press,1986),pp.3-14.
3) Macklin, W. C. and Hobbs, P. V., Surface Phenomena and the Splashing of Drops on Shallow Liquids. Science, 166(1969), pp.107-108.
4) Amsden, A. A. and Harlow, F. H., The SMAC method: A numerical technique for calculating imcompressible fluid flow. (Los Alamos Scientific Laboratory Report, 1970) LA-4370.

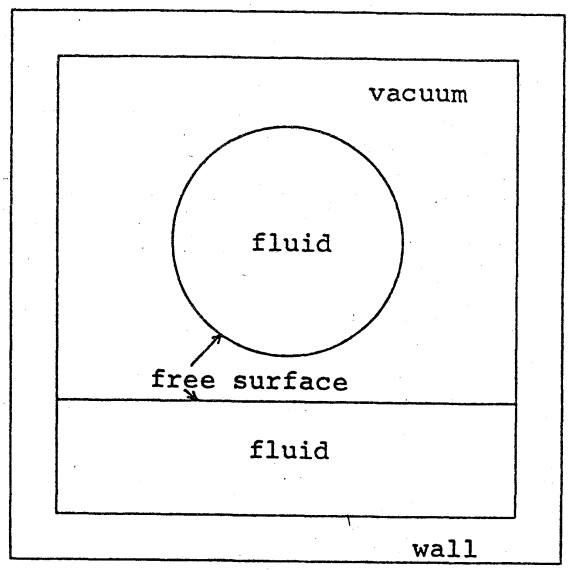

Fig.1.a

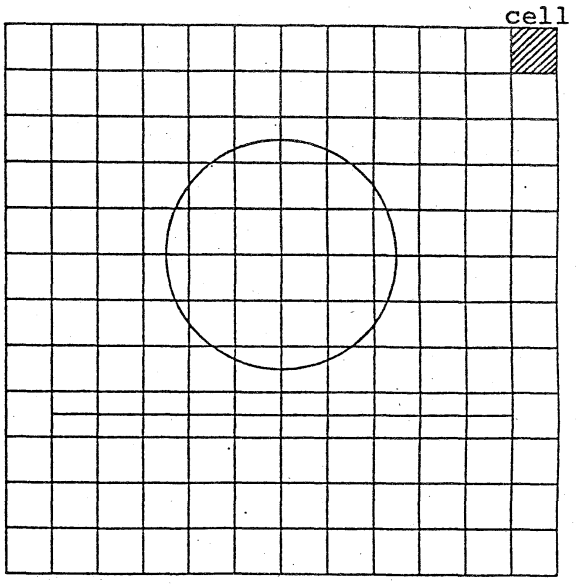

Fig.1.b

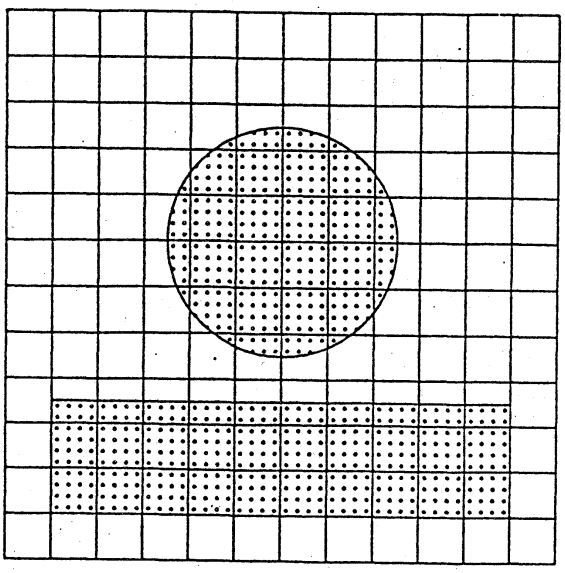

Fig.1.c

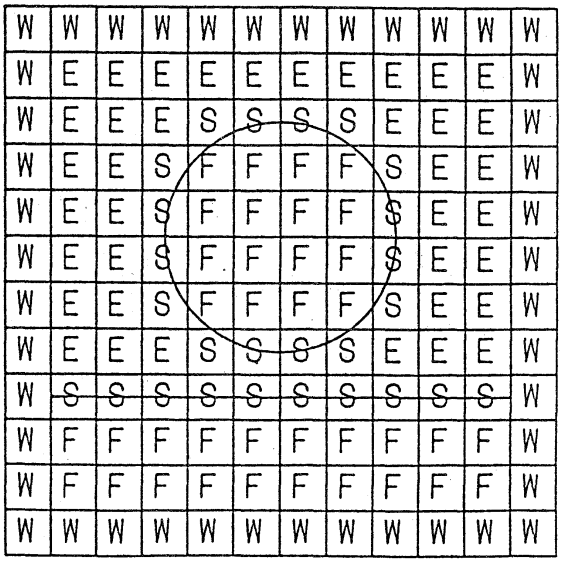

Fig.1.d

FIG.1:Conceptional figures of MAC method.

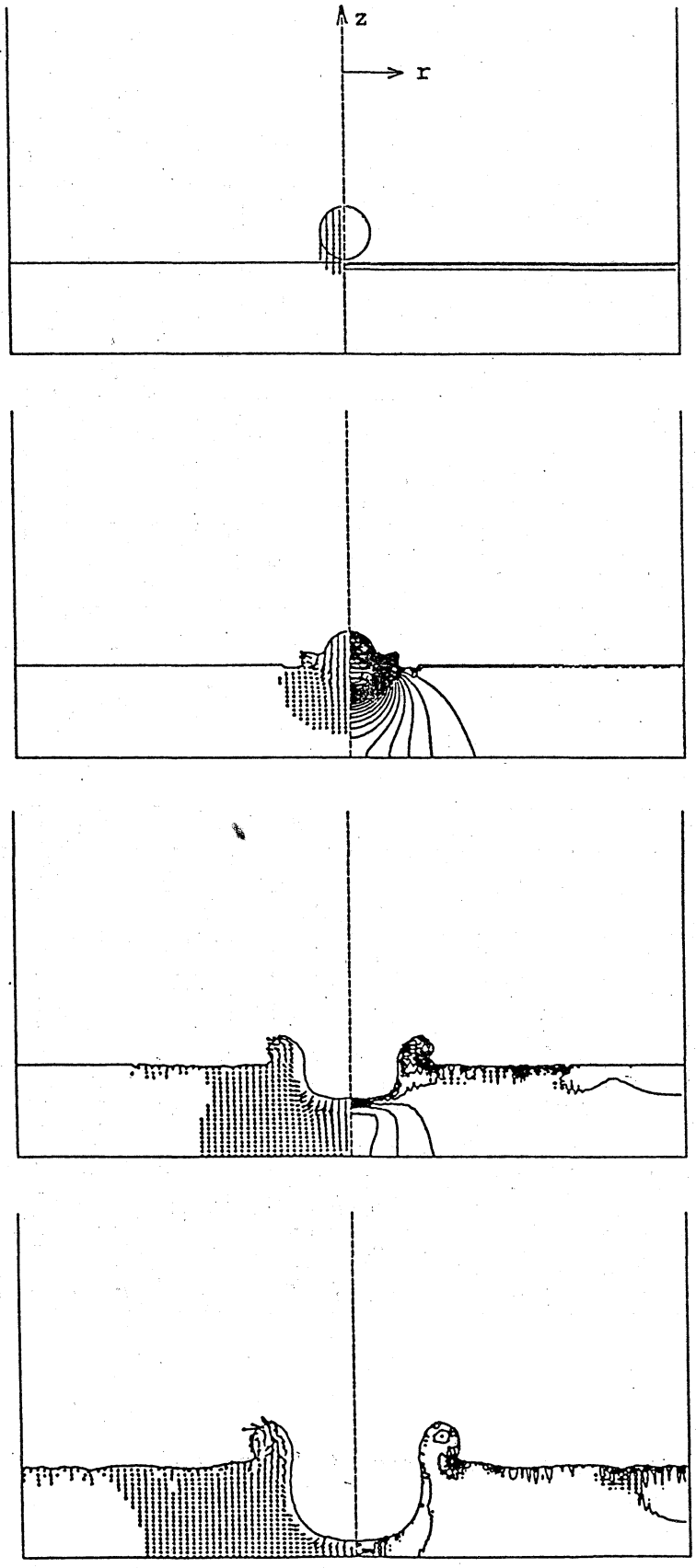

Fig.2:Splashing of a droplet into a pool.

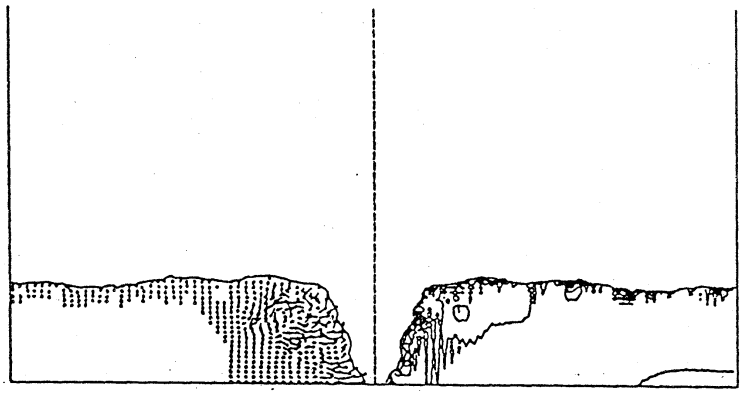

$T=21.6\times10^{-3}$

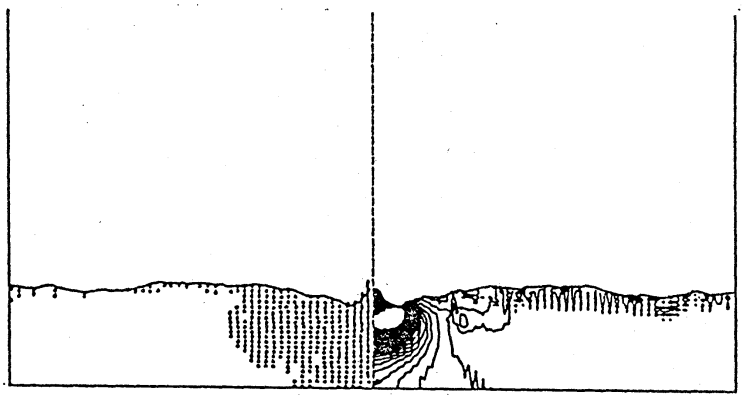

$T=23.2\times10^{-3}$

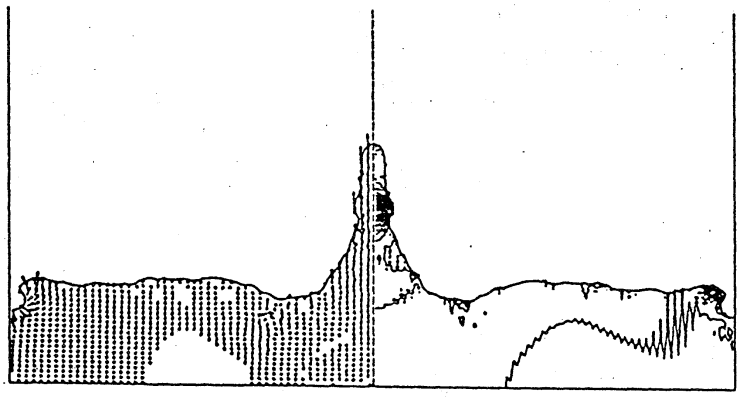

$T=27.2\times10^{-3}$

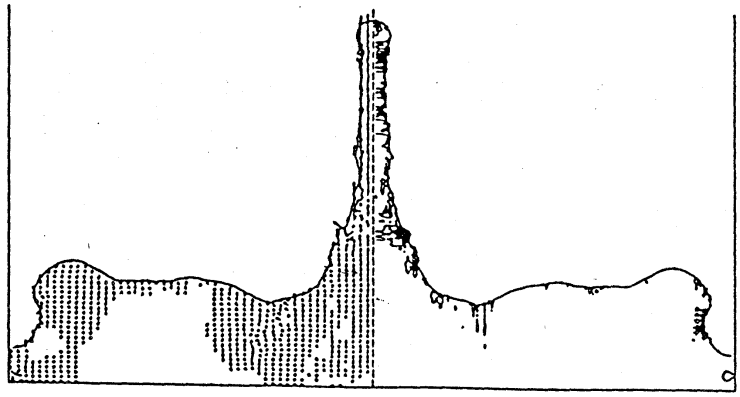

$T=32.6\times10^{-3}$

Fig.2 (continued)

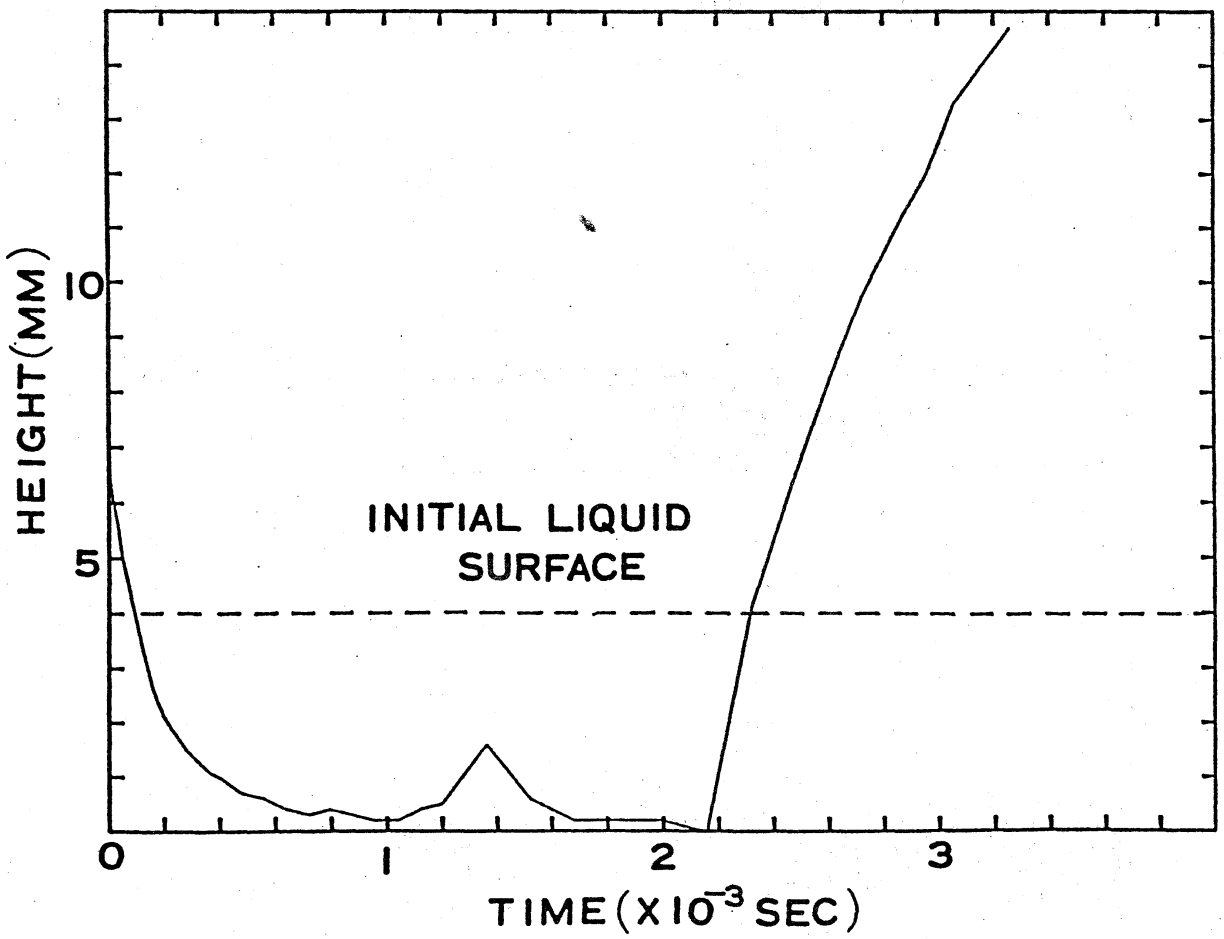

Fig.3:Dependence of a maximum height of the liquid region on the symmetry axis on time.

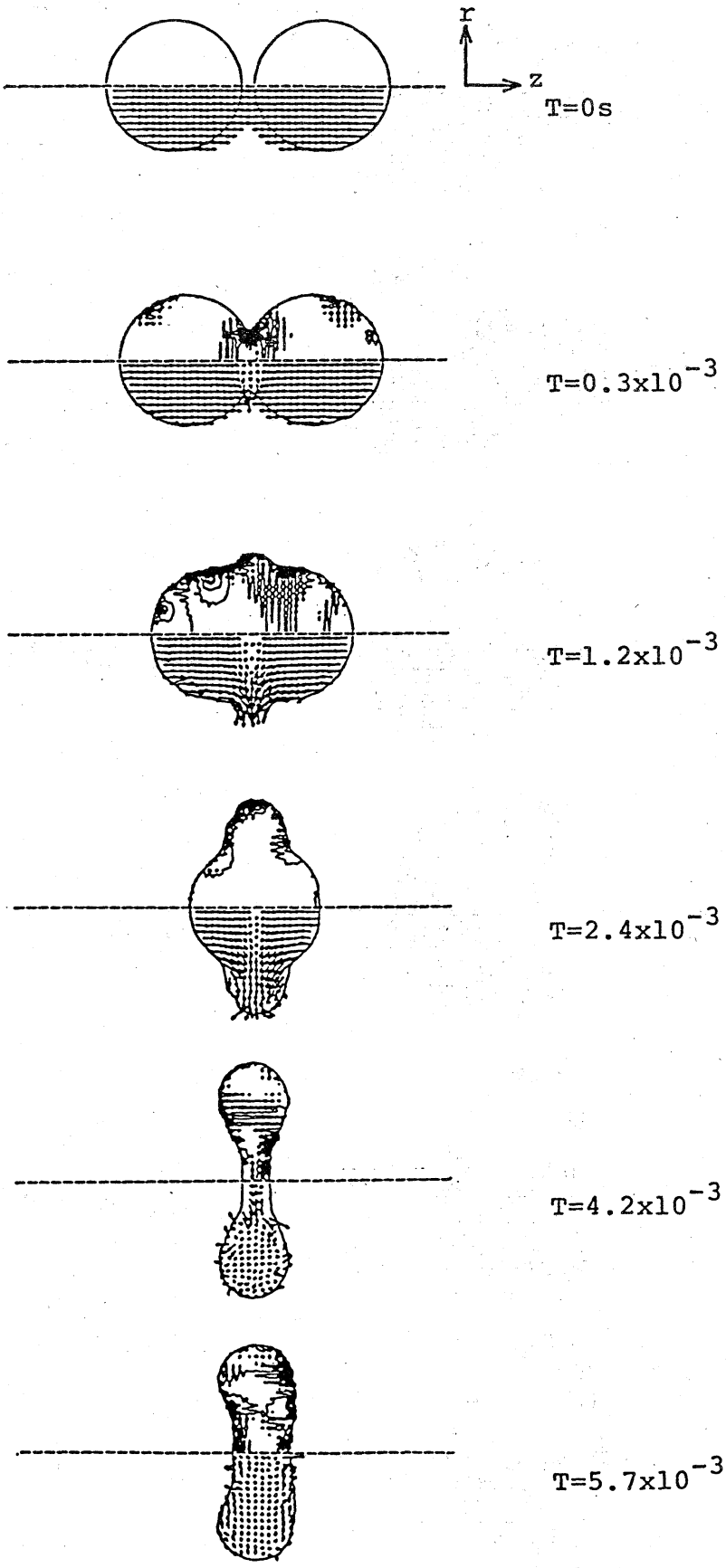

Fig.4:Axisymmetrical collision of droplets.

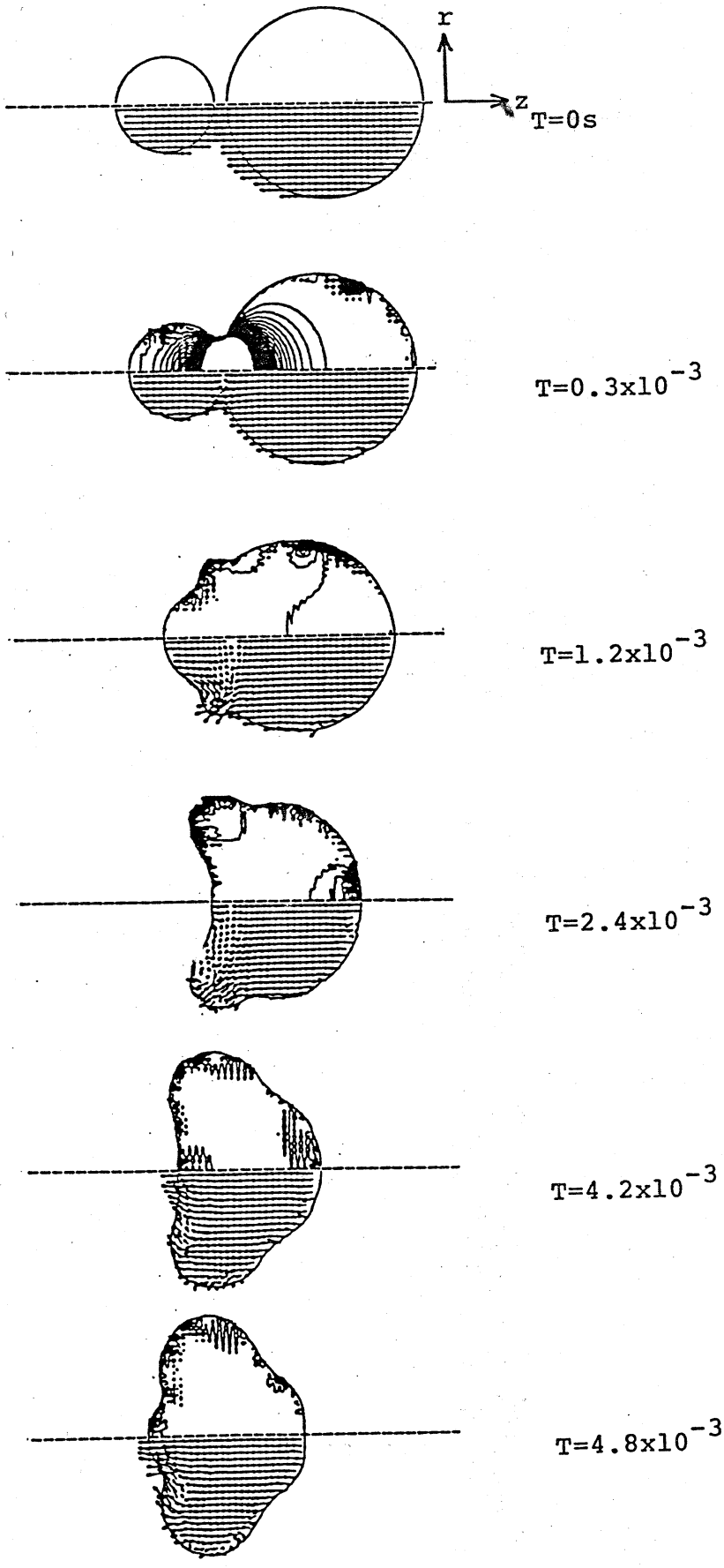

Fig.5:Axisymmetrical collision of droplets.

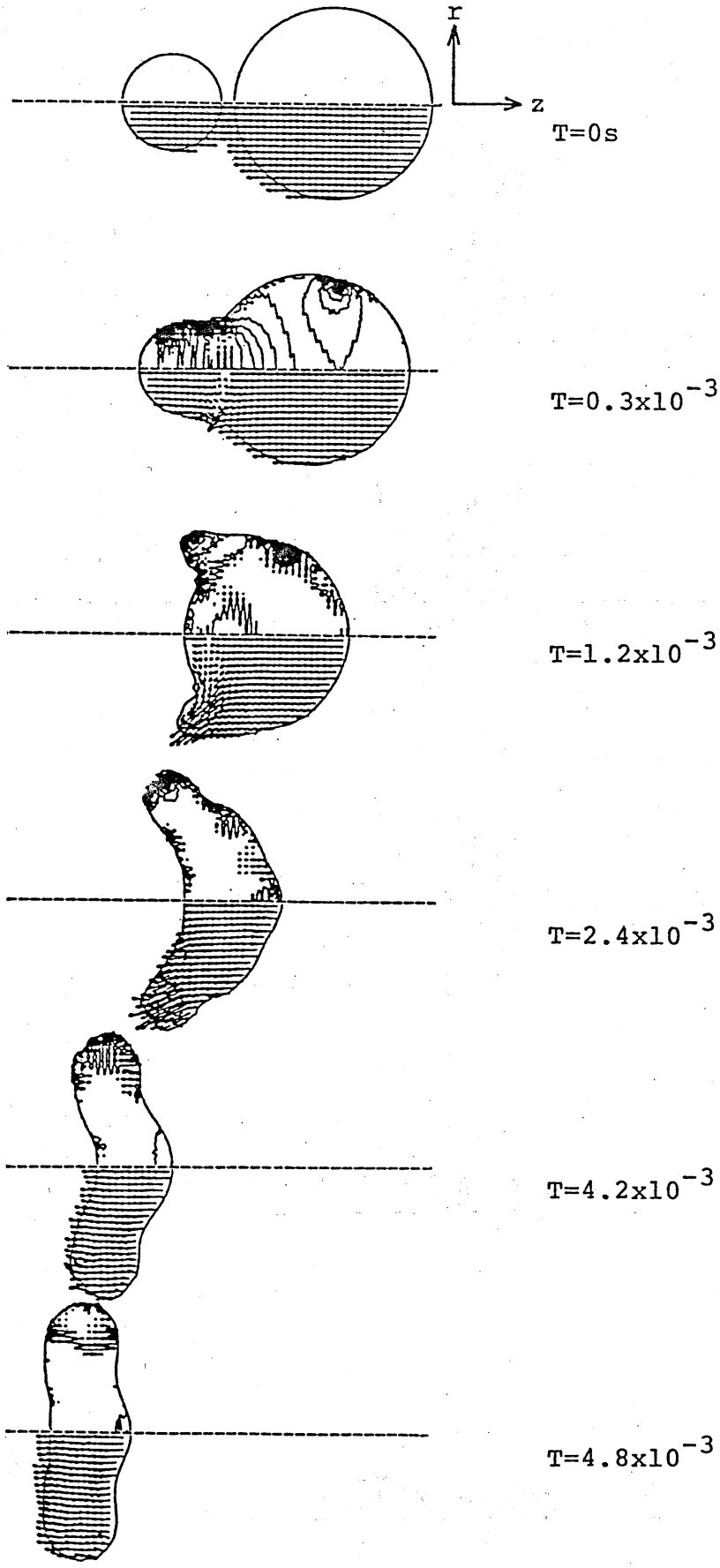

Fig.6: Axisymmetrical collision of droplets.

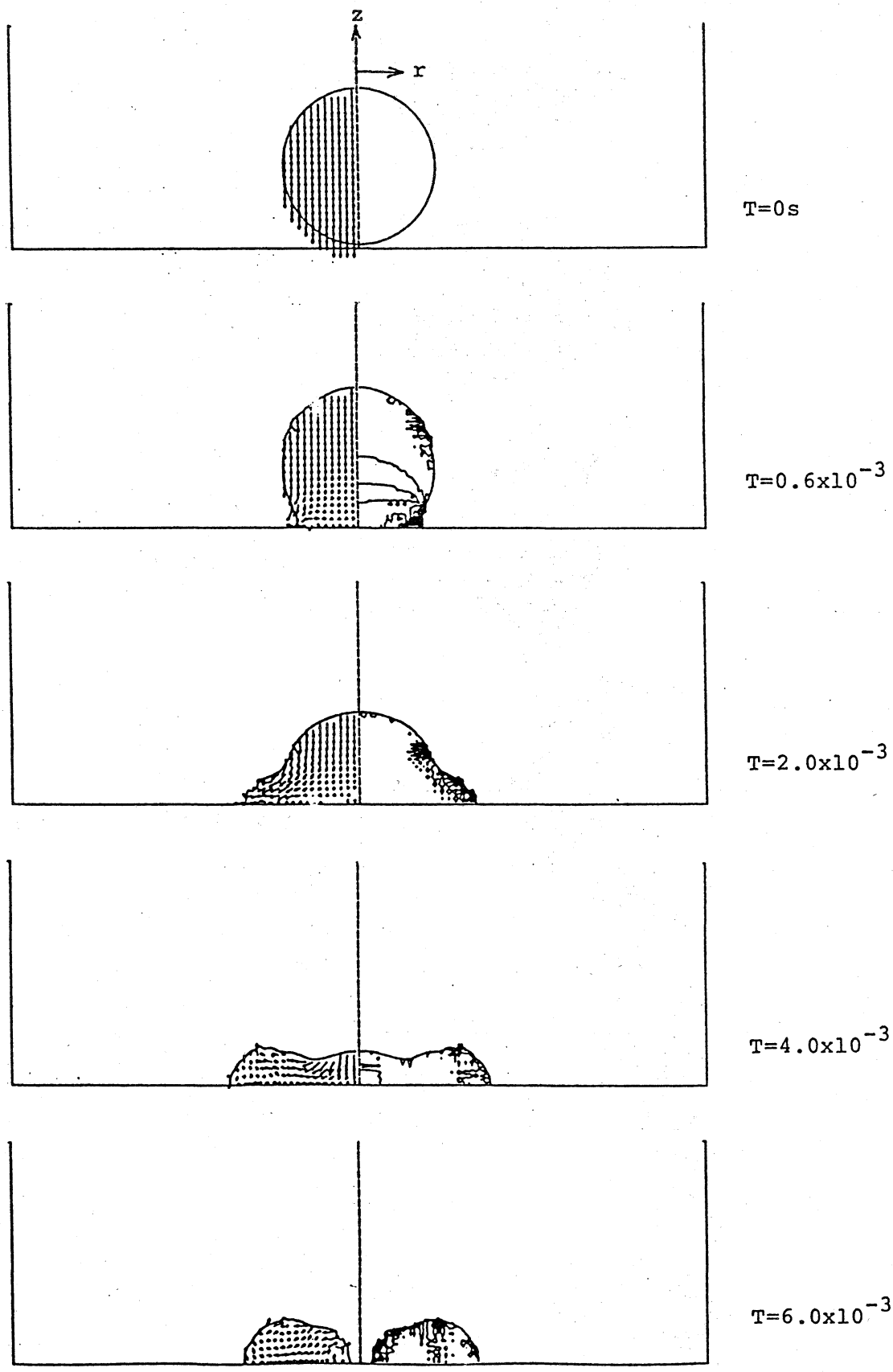

Fig.7:Axisymmetrical collision of a droplet with a rigid wall.

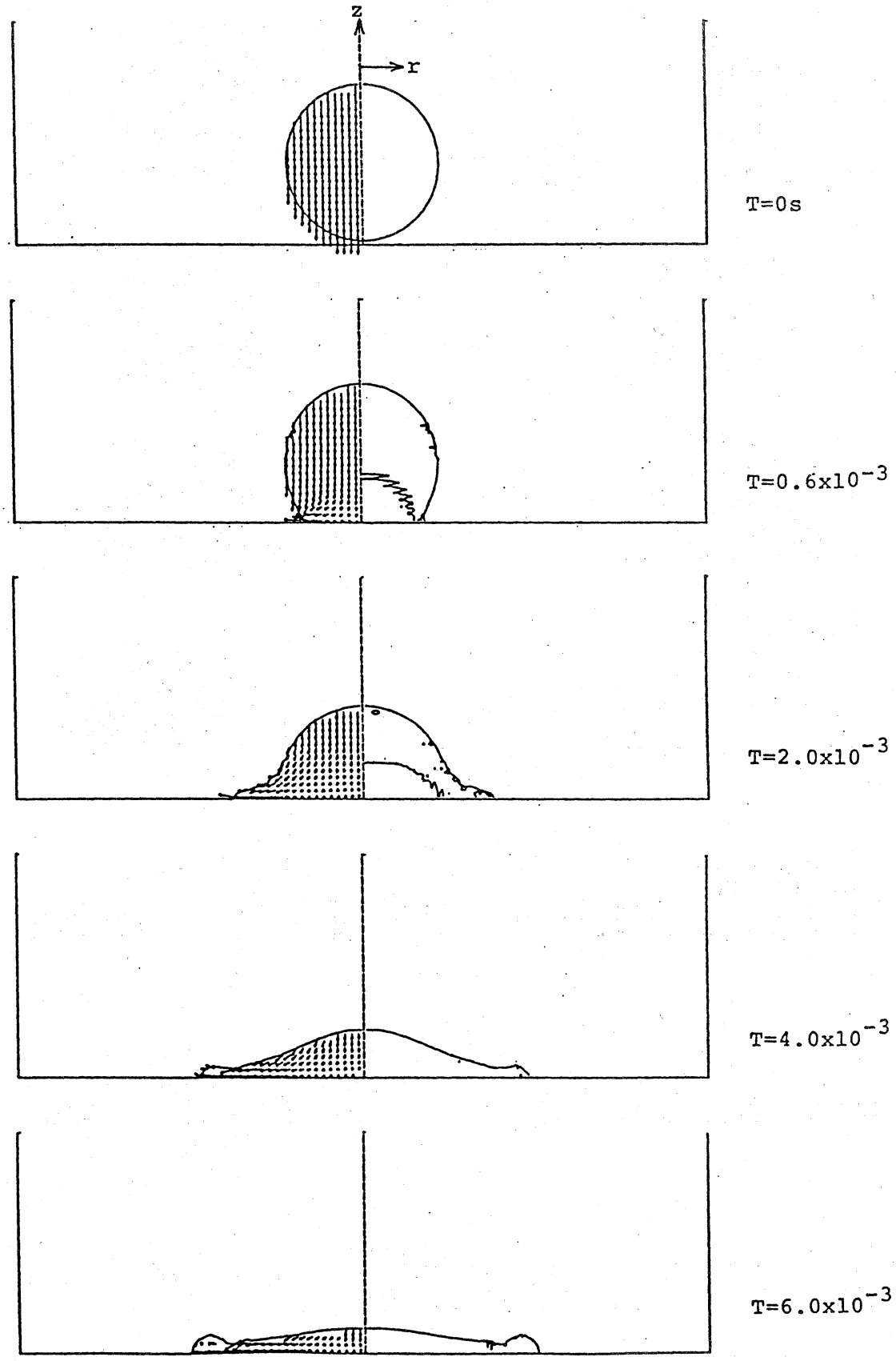

Fig.8:Axisymmetrical collision of a droplet with a rigid wall.

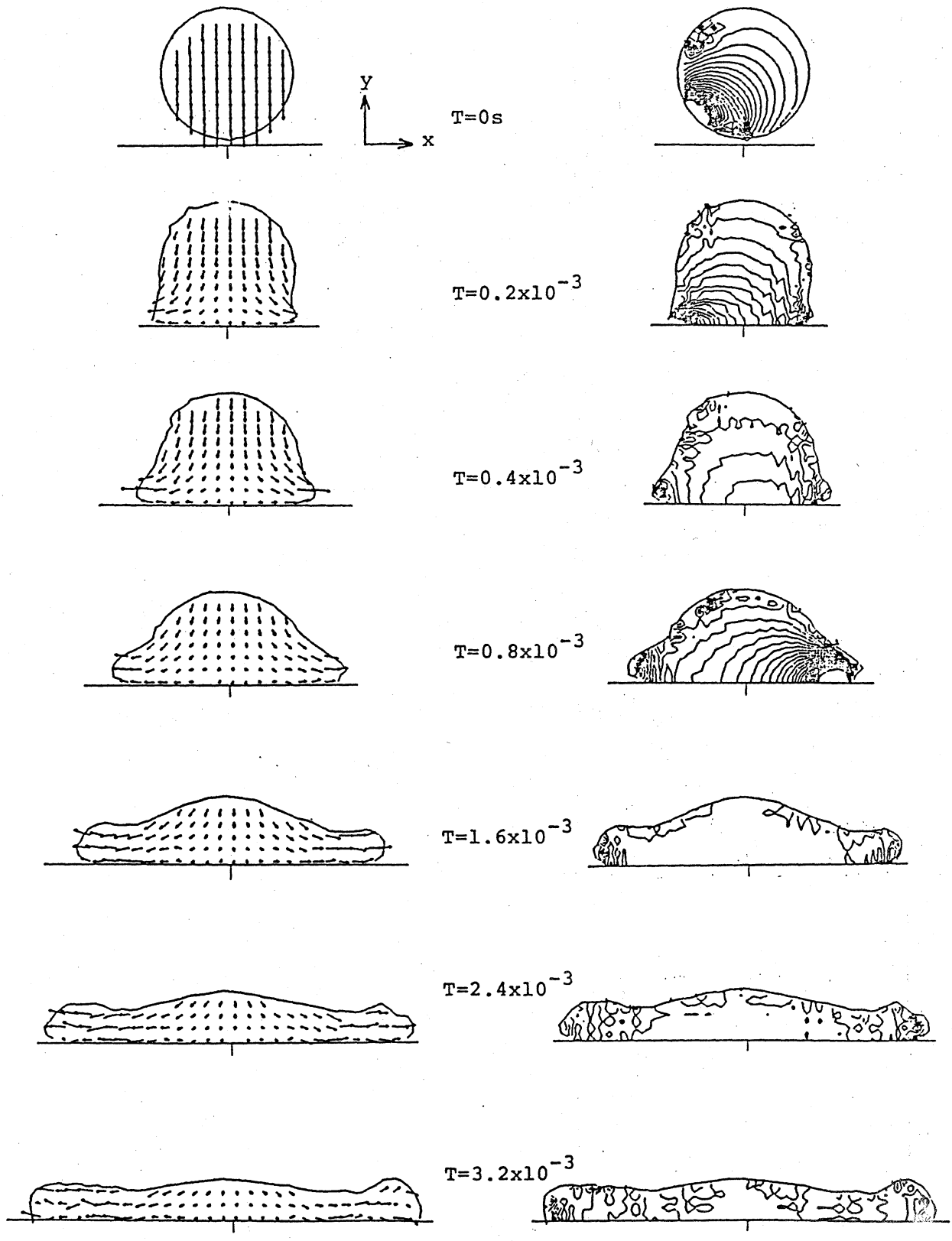

Fig.9:Two-dimensional collision of a droplet with a rigid wall.

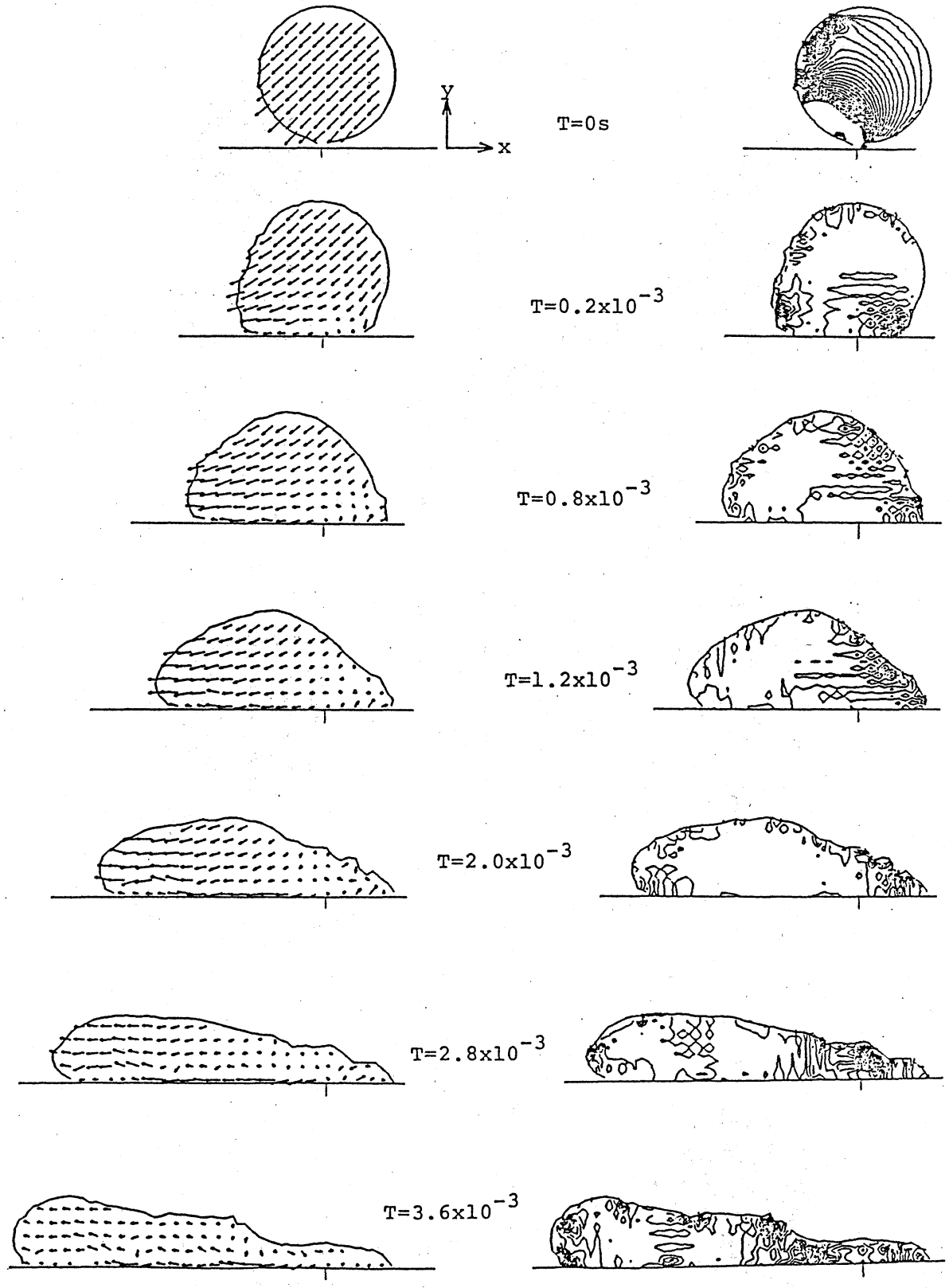

Fig.10:Two-dimensional collision of a droplet with a rigid wall.

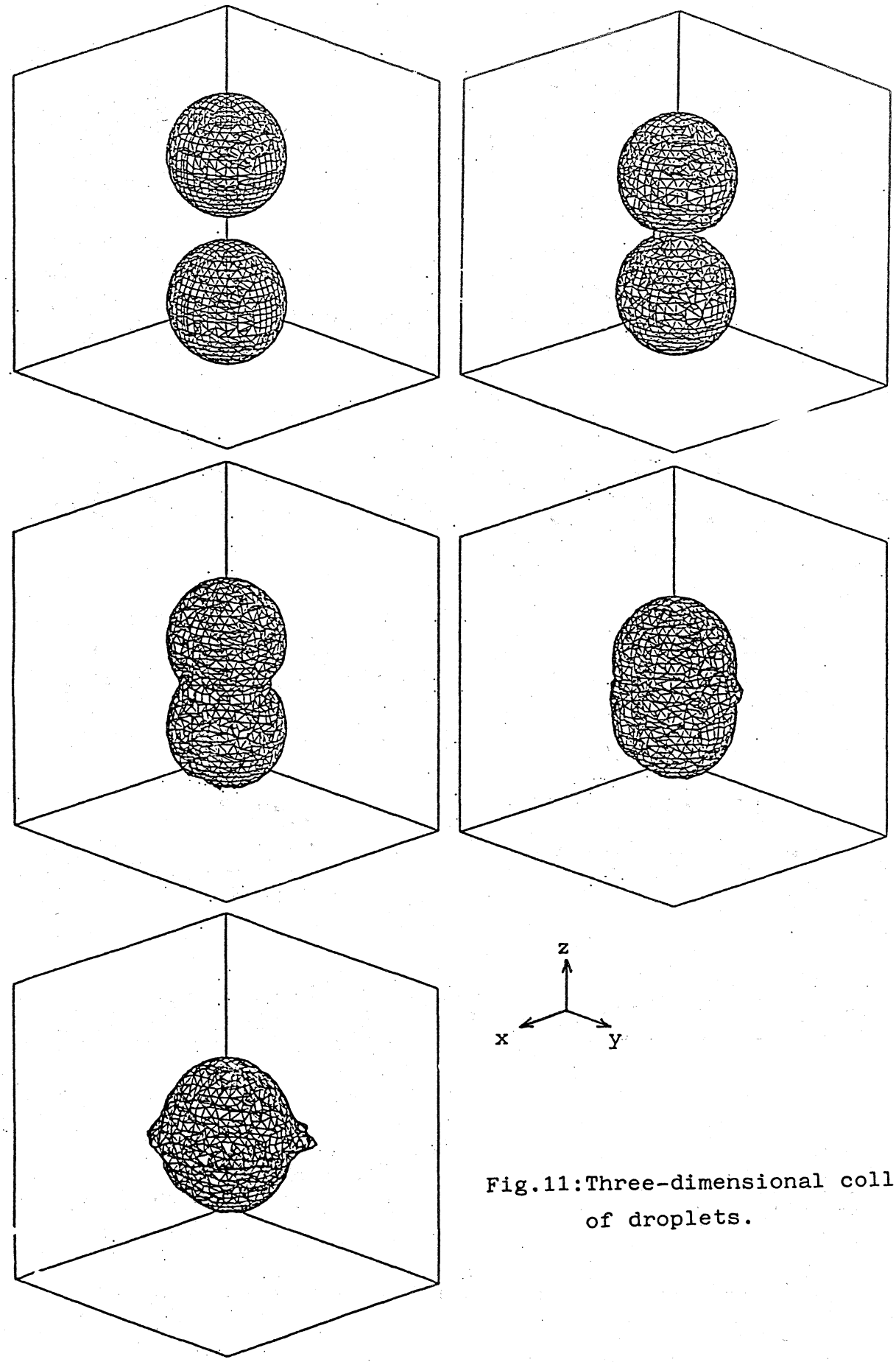

Fig.11:Three-dimensional collisio
of droplets.

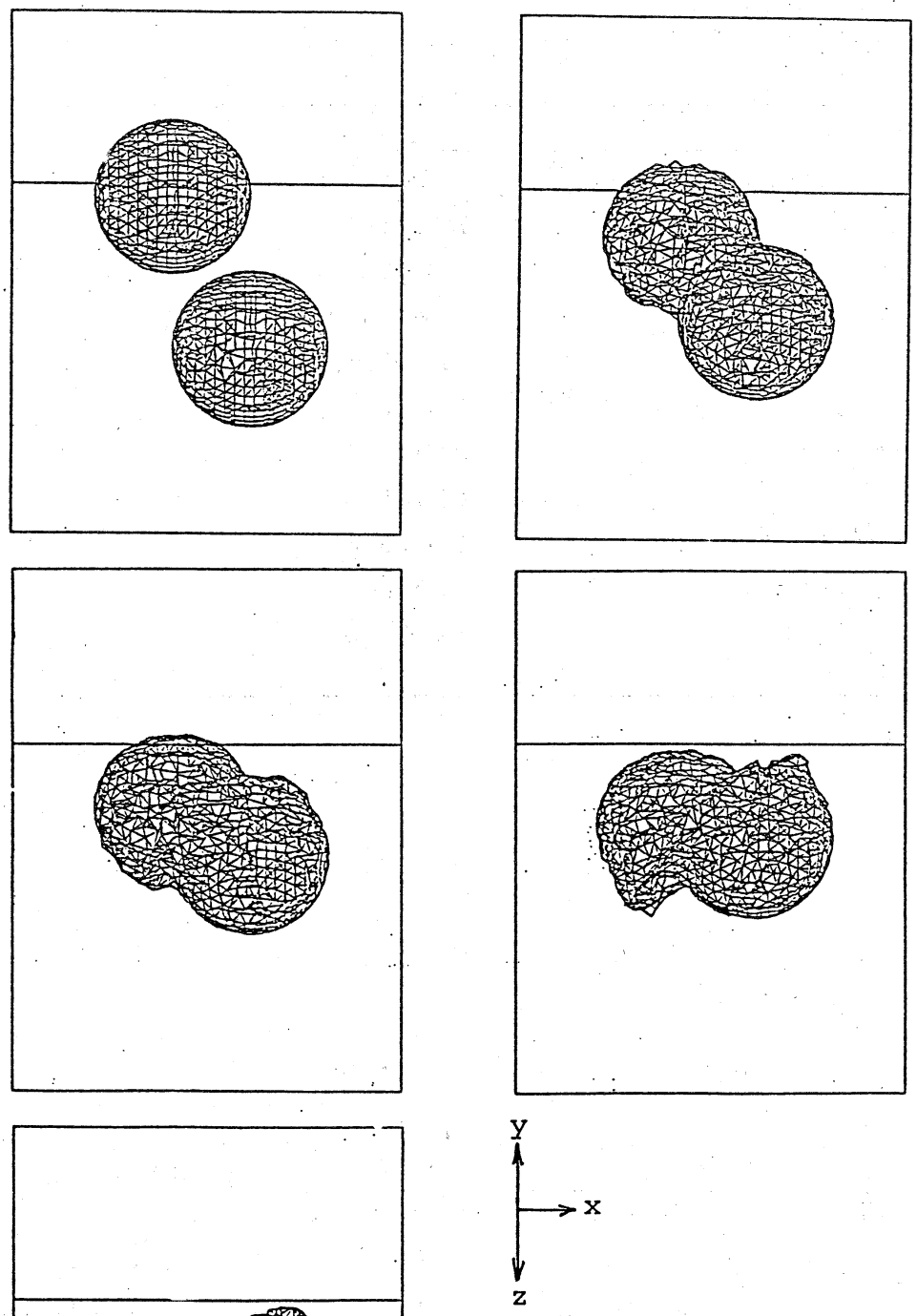

Fig.12: Three-dimensional collision of droplets.

Table 1:Splashing of a droplet.

	Fig.2
kinematic viscosity	$0.01cm^2/s$
surface tension	75dyn/cm
diameter of a droplet	0.23cm
velocity of a droplet	-320cm/s
gravity	$-1000cm/s^2$
depth of a pool	0.4cm
diameter of a pool	3.0cm
mesh size	100x100
mesh interval(Δr)	0.015cm
mesh interval(Δz)	0.01cm
time interval(Δt)	$4x10^{-6}s$

Table 2:Axisymmetrical collision of two droplets.

	Fig.4	Fig.5	Fig.6
kinematic viscosity	$0.01cm^2/s$	$0.01cm^2/s$	$0.01cm^2/s$
surface tension	75dyn/cm	75dyn/cm	75dyn/cm
diameter of droplets	0.2cm,0.2cm	0.3cm,0.15cm	0.3cm,0.15cm
velocity of droplets	$\pm$50cm/s	$\pm$50cm/s	$\pm$100cm/s
mesh size	130(z)x80(r)	130(z)x80(r)	130(z)x80(r)
mesh interval(Δr)	0.005cm	0.005cm	0.005cm
mesh interval(Δz)	0.005cm	0.005cm	0.005cm
time interval(Δt)	$1x10^{-6}s$	$1x10^{-6}s$	$5x10^{-7}s$

Table 3:Axisymmetrical conllision of a droplet with a rigid wall.

	Fig.7	Fig.8
kinematic viscosity	$0.01cm^2/s$	$0.01cm^2/s$
surface tension	75dyn/cm	15dyn/cm
diameter of a droplet	0.22cm	0.22cm
velocity of a droplet	-50cm/s	-50cm/s
mesh size	100x100	100x100
mesh interval(Δr)	0.005cm	0.005cm
mesh interval(Δz)	0.005cm	0.005cm
time interval(Δt)	$1x10^{-6}s$	$1x10^{-6}s$

Table 4:Two-dimensional collision of a droplet with a rigid wall.

	Fig.9	Fig.10
kinematic viscosity	$0.01cm^2/s$	$0.01cm^2/s$
surface tension	75dyn/cm	75dyn/cm
collision angle	90^o	45^o
diameter of a droplet	0.22cm	0.22cm
velocity of a droplet	-50cm/s	-50cm/s
mesh size	100x100	100x100
mesh interval(Δx)	0.005cm	0.005cm
mesh interval(Δy)	0.005cm	0.005cm
time interval(Δt)	$1x10^{-6}s$	$1x10^{-6}s$

Table 5:Three-dimensional collision of two droplets.

	Fig.11	Fig.12
kinematic viscosity	0.01cm^2/s	0.01cm^2/s
surface tension	75dyn/cm	75dyn/cm
diameter of droplets	2cm,2cm	2cm,2cm
velocity of droplets	$\pm$500cm/s	$\pm$500cm/s
initial position of	(2.5,2.5,1.25)	(2.0,2.5,1.25)
centers of droplets(cm)	(2.5,2.5,3.75)	(3.0,2.5,3.75)
mesh size	40(x)x40(y)x50(z)	40(x)x40(y)x50(z)
mesh interval(Δx)	0.125cm	0.125cm
mesh interval(Δy)	0.125cm	0.125cm
mesh interval(Δz)	0.1cm	0.1cm
time interval(Δt)	2x10^{-5}s	2x10^{-5}s